

# Processing optimization of spin crossover materials in large-area molecular junctions

---

Timen Jansma

1903705

## Research group:

Molecular Electronics – Physics of Organic Semiconductors  
(MEPOS)

## Supervisors:

drs. Ilias Katsouras

prof. dr. Dago de Leeuw

## **Abstract**

Bistable spin crossover (SCO) materials are interesting candidates for molecular electronics due to their potential use as switches. The interplay between magnetic properties and electrical transport is of particular importance, but has not been investigated at length. In this research we address the spin crossover material trans-[Fe(babpy)(NCS)<sub>2</sub>]. We develop a method for making a uniform thin film of this material using solution processing and the technique of spin coating. The electrical properties of trans-[Fe(babpy)(NCS)<sub>2</sub>] are studied in large-area molecular junctions.

## Contents

|                              |    |
|------------------------------|----|
| Abstract .....               | 1  |
| Introduction.....            | 3  |
| Theory.....                  | 4  |
| Materials and Methods .....  | 5  |
| Results and Discussion ..... | 9  |
| Conclusions.....             | 15 |
| Acknowledgments.....         | 15 |
| References.....              | 16 |

## Introduction

Computational power and data storage are big issues in the modern world. Technology of today is continuously looking for new ways to increase the number of transistors on integrated circuits. In 1965 Gordon Moore made the prediction that this number would double approximately every two years.<sup>1</sup> This implies that the size of one transistor will halve in that same time. The prediction turned out to have a great reliability, but it is believed even by Moore himself that this growth will eventually reach a limit.<sup>1</sup>

A typical transistor is made using inorganic semiconductors, mostly silicon. Silicon is used because it is cheap to process, it can operate at high speed, and is very reliable.<sup>2</sup> As transistors are becoming smaller and smaller, it becomes increasingly challenging to process this inorganic semiconductor. In a technological device, such as a computer, it is necessary that all transistors are functioning. Failure of one transistor can cause the malfunctioning of the whole machine.<sup>2</sup> Smaller transistors require the manufacturing procedure to be more precise, to ensure that the transistors have a high reproducibility and yield. In addition, sizes of transistors might become so small that quantum mechanical aspects come into play,<sup>3</sup> making processing at smaller scales even more challenging.

Because decreasing transistor size becomes increasingly difficult, looking for new ways and other materials could be beneficial. A possible answer for extending the trend of Moore's Law even further might lie in the field of *molecular electronics*. Molecular electronics studies the possibilities for creating electronic components using organic materials such as polymers and small molecules. By connecting to a single molecule, one could make electrical components with sizes not far from that of a single atom. One of the big challenges for molecular electronics is finding materials with the right properties, suited for use, for example, as a molecular (optical) switch<sup>4</sup>, memory<sup>5</sup> or diode<sup>6</sup>.

Connecting to a single molecule is not a trivial task. Several methods have been employed. It has been achieved by attaching the molecule with covalent bonds to two or more electrodes, but controlling the contact of the molecule with the electrodes proved difficult, leading to a low degree of reproducibility.<sup>7</sup> Another example of a technique used, is to produce electrodes spaced by a molecular sized gap; attached to the molecule are groups that are able to form a bond with the electrodes, so that the molecule can bridge the gap.<sup>7</sup> Here, controlling the gap size between the electrodes was particularly challenging.<sup>7</sup>

In this work we use the technology of large-area molecular junctions, previously developed for the electrical characterization of self-assembled monolayers (SAMs).<sup>8</sup> Using a silicon wafer as substrate, this technology allows for a self-assembling layer of one molecule thick to be formed onto a bottom contact, in a pattern that is defined by a layer of photoresist. On top of the sample, a layer of the highly conducting PEDOT and a top contact is placed.<sup>8</sup> This way, a uniform layer with the thickness of only one molecule can be electrically addressed. This versatile experimental testbed can be used to access the transport properties not only of self-assembled monolayers of molecules, but of thin films of polymers and small molecules as well.

In this research we investigate a material that possesses potentially interesting qualities. Trans-[Fe(bapbpy)(NCS)<sub>2</sub>] is an iron(II)-based molecule that has spin crossover properties, making it potentially suitable as a molecular switch. Spin crossover materials have two spin states: a high spin state and a low spin state. Switching between these two states can be done by using various external stimuli such as temperature, pressure, illumination and magnetic field. The goal of this research is to investigate whether or not it is possible to switch our material between low and high spin state by applying an electric field. This method has not been studied extensively, making it an interesting topic where a lot of insight on the properties of spin crossover materials and their applications in molecular electronics can be gained.

In this report we examine the optimal experimental procedure for producing a layer of this material, which is suitable for electrical measurements in large-area molecular junctions. Afterwards a study on the electrical properties is performed, showing the IV-characteristics of the material.

## Theory

### Spin Crossover

Materials having spin crossover (SCO) properties possess two spin states: a high spin state (HS) and a low spin state (LS). In the high spin state the total magnetic spin of the electrons of the molecule is higher than in the low spin state. The spin crossover effect originates from the splitting of the d-orbital of a metal complex,<sup>9</sup> which consists of a metallic atom or ion with molecules or anions attached to it. These molecules and anions are in turn called 'ligands'. The 'ligand field' describes the orbital characteristics of the metal complex.

The magnitude of the ligand field splitting along with the pairing energy of the complex determines whether it will have a LS or HS electron configuration.

In low spin state, the splitting of the ligand field (or 'orbital splitting') is greater than the pairing energy of the complex. Since a substantial amount of energy is required for the electrons to overcome the energy gap, they remain paired, complying with Hund's Rule, so that the total spin  $S = 0$ .<sup>10</sup>

For the high spin state, the orbital splitting is narrower. The energy required to populate the higher levels is less than the pairing energy and the electrons populate the higher energy orbitals before pairing with electrons in the lower lying orbitals, resulting in a higher total spin.

Figure 1<sup>11</sup> shows a schematic representation of these two cases. A well-known example of SCO occurs in metal complexes with a  $3d^4-3d^7$  electron configuration,<sup>12</sup> where the metal core is surrounded by ligands in an octahedral formation; it is this configuration that our material,  $\text{trans-}[\text{Fe}(\text{bapbpy})(\text{NCS})_2]$ , possesses.

Switching between the two states in SCO materials can be triggered by external

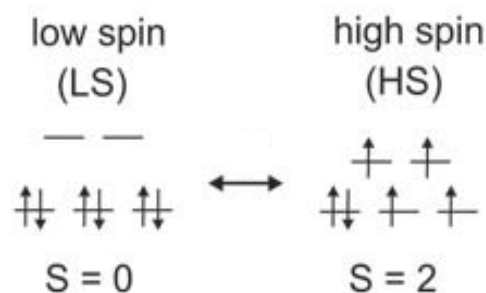


Figure 1. Low spin and high spin

stimuli such as temperature, pressure, illumination and magnetic field. These processes are well-understood.<sup>11</sup> In general, there are three types of transitions, as showed in figure 2<sup>13</sup>: a gradual transition (A), a transition showing a hysteresis loop (B), and a two-step transition (C). The figure shows these three types, where, as an example, the percentage of the material in high spin state is shown as a function of temperature. For the transition showing hysteresis effects, the LS-to-HS transition occurs at a higher temperature than the HS-to-LS transition. The abrupt changes for this type indicate that the metal complexes cooperate; a transition of one complex triggers the transition of other complexes. Two-step transitions, which are not very common, might indicate just the opposite: the transition of a metal complex counteracts transitions of others.<sup>13</sup> The intermolecular interactions might originate in the elasticity of the material. As a result of the spin transition, bond lengths of the ligands change, which causes alteration of the structure of the metal complex. This effect can induce lattice strains, causing long-range interactions. The stable intermediate step of the two-step transition might be a result of

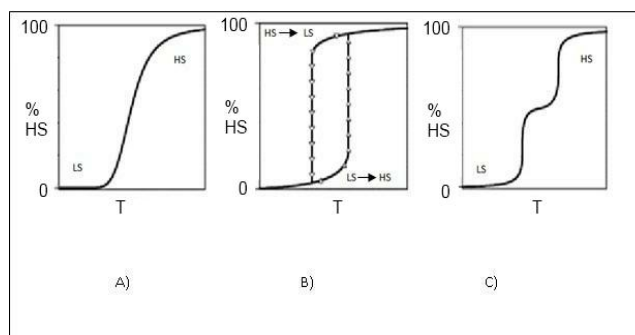


Figure 2. Three types of spin transition: (A) a gradual transition, (B) a transition showing a hysteresis loop, and (C) a two-step transition

the formation of nearest-neighbor LS-HS pairs.<sup>10</sup>

Magnetic susceptibility is a proportionality constant, that shows the degree of magnetization of the material when an external magnetic field is applied. With the higher spin number in high spin state, this magnetization is higher than for low spin state, resulting in a higher magnetic susceptibility. This can be used to acquire the transition characteristics as those in figure 2.

Due to changes in the 3d electron configuration, the complex structure can undergo considerable changes, resulting in differences of its size and color when a spin transition takes place. In bulk samples this could result in changes of the volume of the material. The dielectric and mechanical properties can vary also.<sup>12</sup>

With the eye on electronics, transitions showing hysteresis properties are of particular interest, as there exist external circumstances where the material is bistable: depending on the history, the material is either in low spin state or in high spin state. This is especially interesting when the hysteresis region occurs around room temperature. If there is a way to actively choose the state of the metal complexes, the material could potentially be used as a switch or as data storage medium. However, in order to use the material in an electrical component, reading the stored information is possible only when the material has a different conductivity in the two spin states. If the two spin states have the same conductivity, there is no way of distinguishing between the two states electrically. If the spin state itself can also be controlled electrically, it presents good prospects for integration in electronics.

In 2011, F. Prins *et al.* succeeded in producing a spin crossover system showing bistability and hysteresis effects at room temperature by applying a voltage bias.<sup>11</sup> They accomplished this by creating nanoparticles covered with the SCO material and placing them between two gold electrodes separated by approximately 5-10 nm.

Using molecules as a material for electrical components has the advantages that transitions can be obtained at molecular scale, possibly around room temperature, and the

switching of the molecules occurs at very high speed.<sup>12</sup> Furthermore, the possibilities for designing new materials are virtually endless.<sup>12</sup>

The SCO properties are highly dependent on the structure of the ligands. However, it is becoming evident that the interactions between the molecules also have a large effect on the macroscopic properties of the material.<sup>14</sup> As these interactions cannot be accurately predicted, a lot of processing experiments have to be done for every compound to optimize the SCO properties.<sup>14</sup> It is of particular interest to investigate the scaling properties of the spin crossover effect and its dependence on the layer thickness.

## Materials and Methods

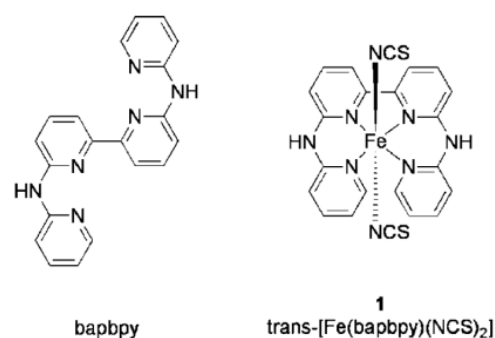
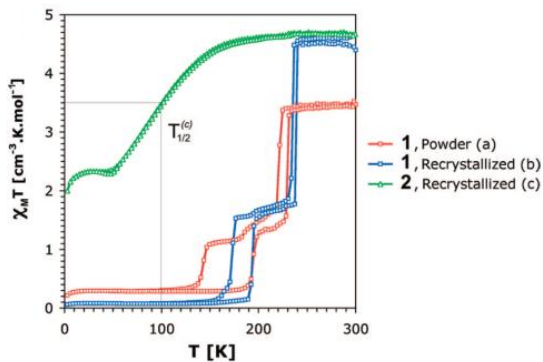


Figure 3. Structure of the bapbpy ligand (left), and structure of trans-[Fe(bapbpy)(NCS)<sub>2</sub>] (right)

### The material

The material used in this research, trans-[Fe(bapbpy)(NCS)<sub>2</sub>], is a small molecule based on iron(II). The structure of this molecule is shown in figure 3<sup>14</sup>. The iron(II) nucleus is located in the center. Bonded to it are two NCS groups, and a tetradentate ligand called 'bapbpy' is attached around it.<sup>14</sup>

The material, as well as the bapbpy ligand, is synthesized by S. Bonnet *et al.*, who investigated the material's spin crossover properties using powder X-ray diffraction, Mössbauer spectroscopy, Raman spectroscopy, calorimetry and magnetic susceptibility measurements.<sup>14</sup> The results of the latter experiment, involving measurements of the magnetic susceptibility



**Figure 4. Magnetic susceptibility measurements for  $\text{trans-[Fe(bapbpy)(NCS)}_2\text{]}$  processed in 3 different ways**

as a function of temperature, are shown in figure 4<sup>14</sup>. Here  $\chi_M$  is the molar magnetic susceptibility and  $T$  is the temperature. Figure 4(a) shows measurements performed on the crude powder attained after synthesis. In figure 4(b), the material was dissolved in a mixture of DMF (dimethylformamide) and methanol, and recrystallized, leaving a polycrystalline sample. Same procedure was followed for the measurements shown in figure 4(c), only here a mixture of DMF and diisopropylether was used<sup>14</sup>.

These results exemplify the fact that processing methods are highly influencing the SCO properties of an SCO material. When processed as (a) and (b) in figure 4, the material shows a two-step transition and hysteresis properties below room temperature. The steep transitions, and the two-step characteristics, indicate pronounced interactions between the complexes.<sup>14</sup> When the material is recrystallized in a mixture of DMF and diisopropylether, however, a crystal that shows a gradual transition in the 50 K to 200 K region is obtained, with a high portion already in high state close to 0 K (figure 4(c)).

In this research we retrieve a solid state of the material, in the form of a thin film, after dissolving it in DMF (further details about this will be discussed in this chapter's subsection 'Making a layer of the SCO material'). Since we use pure DMF as a solvent, unlike the procedures described in figure 4, we do not know what the structure of the bulk material will be, and therefore have no prior knowledge of the magnetic susceptibility properties.

We will investigate whether or not it is possible to switch between low and high spin state using an electric field.

### *The large-area molecular junction*

In this research we employ the experimental testbed of large-area molecular junctions to measure the electrical properties of our material. The architecture of the large-area molecular junctions is developed by H. Akkerman *et. al.*<sup>8</sup> Although it is originally developed for measuring self-assembled monolayers (SAMs), it proved to be a versatile testbed, being also suitable for addressing polymers and small molecules. It consists of a number of layers. The configuration used here is shown in figure 5, where the layer 'material' is in our case a thin film of  $\text{trans-[Fe(bapbpy)(NCS)}_2\text{]}$ .

We use pre-manufactured substrates. These were produced by using a silicon substrate with a thermally grown  $\text{SiO}_2$  passivation layer of 500 nm. A titanium adhesion layer was applied, and on top of that a gold contact of 60 nm was evaporated. Subsequently, a highly insulating layer of photoresist was applied by spin coating, a technique discussed in the section 'Making a layer of the SCO material'. Using UV-lithography the layer of photoresist was patterned, creating circular gaps with diameters ranging from 1  $\mu\text{m}$  to 100  $\mu\text{m}$ , on top of the bottom electrodes.

Using these substrates, we can immediately start by applying a layer of our SCO material using the spin coating technique. This layer spreads out over the whole substrate, but the electrical properties are measured only at the locations of the gaps in the photoresist. On top of this layer, a silver top contact is evaporated. To perform



**Figure 5. Structure of the large-area molecular junction, where 'material' indicates the  $\text{trans-[Fe(bapbpy)(NCS)}_2\text{]}$**

electrical measurements a probe is connected to the bottom and the top contact.

### *Making a layer of the SCO material*

The thin films of trans-[Fe(bapbpy)(NCS)<sub>2</sub>] were produced by spin coating inside a glove box. Spin coating is a technique used for acquiring thin films of a material. The material of interest is first fully dissolved in an appropriate solvent. Then, a substrate is placed inside a spin coater, onto a horizontal disk that can rotate around its center axis, called a 'chuck'. With a pipette, a small amount of the solution is placed on the substrate, fully covering it. Then the spin coater is started immediately, before the solvent starts to evaporate. The chuck starts spinning following a predefined program. Due

**Table 1. Details of the two-step spin coater program**

|                             | <i>Step 1</i> | <i>Step 2</i> |
|-----------------------------|---------------|---------------|
| <i>Open/closed cap</i>      | Closed        | Open          |
| <i>Time (s)</i>             | 10            | 60            |
| <i>Speed (rpm)</i>          | variable      | 500           |
| <i>Acceleration (rpm/s)</i> | 500           | 500           |

to the centrifugal force the solution spreads out evenly over the area, and a part of the solution will be accelerated off the substrate. However, as the solvent will be evaporating during the spinning, a small portion of the material will be left behind, leaving a thin film on the substrate. A higher spin coating speed results in a thinner layer, as more of the solution will fly off the substrate. Depending on the properties of the material and the solvent, this film varies in thickness and uniformity as well.

In trying to optimize the processing technique of making a layer, clean glass substrates were used instead of the large-area molecular junctions structure explained above. Each glass substrate was cleaned by

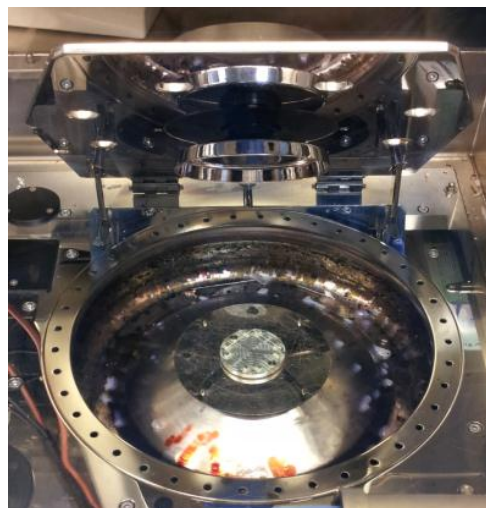


**Figure 6. The spin coater**

first scrubbing its surface with demi water and soap for 2 minutes, which smoothens it by removing spikes on the surface. Then, the samples were consecutively subjected to 5 minutes of rinsing in a demi water flow bath, 5 minutes of ultrasonic cleaning in acetone, again 5 minutes of rinsing in a demi water flow bath, and 5 minutes of ultrasonic cleaning in propanol. The samples were centrifugally dried, and placed in a dust-free container until spin coating.

The trans-[Fe(bapbpy)(NCS)<sub>2</sub>] was received in the crude powder form. The material was dissolved in DMF, as it dissolves best in this solvent, and then the two-step program listed in table 1 was run on the spin coater. The cover could be closed while spin coating, placing a cap over the substrate. The speed of the first step was variable during the experiments, as this step is crucial for the layer thickness. Step 2 was used as a drying phase, to ensure all of the solvent would be evaporated. The cap was opened for this step to speed up the drying process. After 60 seconds the average substrate was dry, except for small spots in the corners. These small wet spots were dried by placing the substrate on a hot plate of 70 °C for approximately one minute, so that they could be safely transferred out of the glovebox.

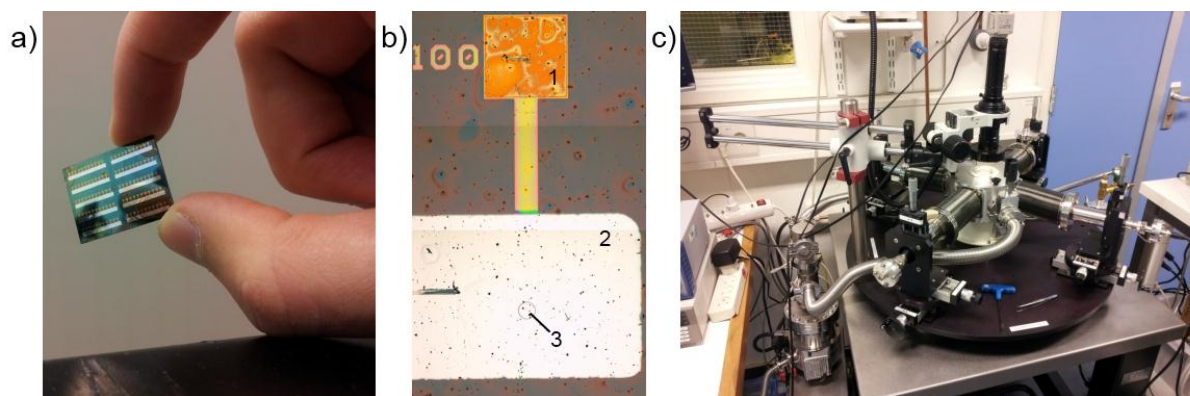


Figure 7. a) A finished wafer containing rows of devices with various hole diameters. b) Microscope picture of one device where (1) is the gold bottom contact, (2) is the silver top contact, and (3) is the hole in the photoresist. c) The probe station.

Multiple parameters were varied and different methods were used in an effort to make smooth uniform layers and optimizing the thickness. These include: varying the concentration of the material in DMF, varying the spin coating speed in step 1, adding polystyrene to the solution, and spin coating on heated substrates.

As the concentration of the solution is increased, a thicker layer is expected: the dependence should be linear in nature. The layer thickness  $D$  can also be controlled by varying the spin coating speed  $\omega$ , as these are inversely square root proportional<sup>15</sup>:  $D \propto \omega^{-0.5}$ . As a next step, to make the layer thicker and/or smoother, we added a small amount of high molecular weight polystyrene. We chose polystyrene, because it is an insulating material that would not interfere with the transport properties of the SCO material during the electrical characterization. This technique of adding a high molecular weight polymer has proved successful in the past, for example in the work of N. Stingelin-Stutzmann *et. al.*<sup>16</sup> Heating the substrates right before spin coating is also tried in order to thicken the layer. When placing the solution on a hot substrate, the solvent evaporates faster, leaving more material behind on the substrate, thereby thickening the layer. This was achieved by placing the substrates on a hot plate for half an hour, heating them to 120°C - close to the boiling point of DMF of 153°C - and transferring them quickly onto the spin coater.

After each batch of spin coated glass substrates, thickness measurements were performed by applying a scratch in the layer using tweezers, a scalpel or a pipette and measuring the profile across the scratch with a Dektak 6 profilometer. This profilometer drags a small stylus over the surface using a very small force. By placing a substrate under the needle and aligning it to measure across a scratch, a detailed profile can be obtained of the surface containing the scratch. Using software, the layer thickness is defined by measuring the average vertical displacement between the locations inside the scratch and outside the scratch.

### *Making devices and measuring IV-characteristics*

When the process of making the layer was optimized, devices were fabricated in large-area molecular junctions. Starting with pre-manufactured silicon wafers with gold contact and patterned photoresist, the material was applied by using the same technique as for the glass substrates. Before this layer was applied, the substrates were cleaned by placing them inside a plasma cleaner for two minutes, and afterwards placing them in ethanol for five minutes. Four substrates were spin coated with the SCO material: two at room temperature, one of which one contained 2% polystyrene, and two at 120°C, one of which contained again 2% polystyrene.

After applying the layer, the top contact, silver, was added using evaporation. The layer thickness of the silver is 100 nm.

A finished substrate is shown in figure 7a. Figure 7b shows a microscope image of one of the devices on a substrate, where (1) is the gold bottom contact, (2) the silver top contact and (3) the gap in the photoresist, in this case with a diameter of 100  $\mu\text{m}$ . The diameter of the holes in the photoresist varied in size from 1  $\mu\text{m}$  to 100  $\mu\text{m}$ .

Electrical measurements on the finished devices were performed by placing the substrates in vacuum in a probe station, shown in figure 7c. There, one probe was connected to the gold bottom contact, and one probe was connected to the silver top contact. In figure 7b the marks of the two probes on the electrodes can still be seen. Using a Keithley 4200 semiconductor analyzer, a voltage sweep bias with a step of 10 mV was applied from 0.0 V to 1.0 V, then lowering to -1.0 V and back to 0.0 V. A dual sweep allows for possible hysteresis effects to be detected. We measure up to 1.0 V, because at higher voltages the risk of breaking the devices would become considerable. When it breaks, it means that the device has become shorted, and measurements cannot be performed anymore. Therefore we chose a relative safe maximum of 1.0 and -1.0 V.

## Results and Discussion

### *Making a layer*

Upon mixing with DMF, the solution is very opaque and bright red, having the same color as the crude powder. This probably means that the material has not yet been dissolved, so that undissolved particles floating can be seen. After leaving it overnight at room temperature and without mixing, the color of the solution has shifted to dark red and is clear, a sign that the material is fully dissolved.

To have an idea what ranges of concentrations should be investigated, it was necessary to know how much trans-[Fe(bapbpy)(NCS)<sub>2</sub>] can be dissolved in DMF. In trying to find the maximum concentration of the SCO material in DMF, we started with making a solution of 10 mg/ml. The next day the material was completely dissolved. We increased the concentration of the solution in steps of 2.5 mg/ml by adding the solid material in the solution, until the solution became oversaturated. At 15 mg/ml, a considerable amount of undissolved trans-[Fe(bapbpy)(NCS)<sub>2</sub>] was observed, whereas at 12.5 mg/ml the solution was completely clear. The maximum concentration of this material in DMF was therefore found to be somewhere between 12.5 and 15 mg/ml. To be sure that the material was properly dissolved, we chose a maximum concentration of 12.5 mg/ml for all further experiments.

Results of varying the concentration and spin coating speed are presented in figure

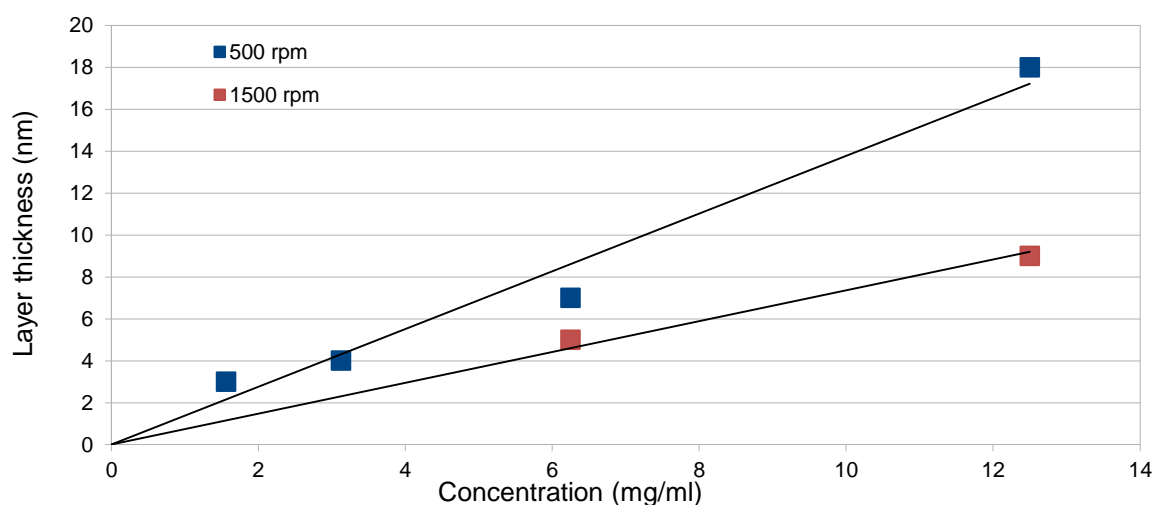


Figure 8. Measurements of layer thickness as a function of concentration, performed at two spin coating speeds: 500 and 1500 rpm.

8. For the lower concentrations of the 1500 rpm batch, it was not possible to determine the layer thickness. Therefore they are not included in the graph. The thicknesses were probably approaching the lower resolution limit of the profilometer.

The data points are showing a linear dependence of the thickness on concentration. As expected, the final layer thickness is reduced when the spinning speed is increased. At the maximum concentration of 12.5 mg/ml and 500 rpm, the layer is approximately 18 nm. Incorporating a layer of such low thickness in the large-area molecular junctions would significantly reduce the yield of functional devices, due to short circuits. Evaporation of metals on top of thin organic layers leads to filamentary growth through the layer. Increasing the spin coater speed is therefore not advantageous. Reducing the speed below 500 rpm, however, is also not an option, as then non-uniformity is starting to become an issue. The best speed for spin coating is therefore 500 rpm. It is also advantageous to use the highest concentration possible, in this case 12.5 mg/ml.

At the edges of the samples, an increase of the thickness was observed, which could also be seen by eye. This effect is probably due to remnant solution at the edges of the substrate during spin coating. While it dries, more trans-[Fe(bapbpy)(NCS)<sub>2</sub>] is left behind on the substrate, locally causing a thicker layer. A run with the profilometer showed that this step is approximately 50 nm thick for the 12.5 mg/ml, 500 rpm sample.

Microscope pictures of the 12.5 mg/ml sample, spin coated at 500 rpm, are shown in figure 9. The pictures include a part of a scratch made for the thickness measurements. The layer is quite smooth and looks uniform. There appear to be some specks on the sample. The solution was not filtered prior to spin coating, so these spots can be due to impurities or small particles of undissolved material.

In an attempt to increase the layer thickness, the technique of adding a high molecular weight polymer was used. The concentration of the material in DMF was lowered to 10.0 mg/ml, so that it would be easier to dissolve the extra polystyrene in the solution. From here on, when polystyrene is added to the solution, the concentration of the SCO in DMF will be 10.0 mg/ml. The rest of the procedure of making a layer has not changed. Figure 10 presents microscope pictures of films spin coated from solutions in which 2% (figure 10 a,b) and 16% (figure 10 c,d) polystyrene has been added. The weight ratio of the SCO material and polystyrene in these samples is therefore 50:1 and 50:8 respectively.

Compared to the samples without any polystyrene, these layers are much less uniform. At low percentages this effect is not very pronounced, but at the high percentage of 16% it becomes very clear that adding polystyrene does not benefit the layer. Furthermore, the effect of the addition of polystyrene on the layer thickness is almost non-existent: the thicknesses stay roughly the same. However, measurements of the

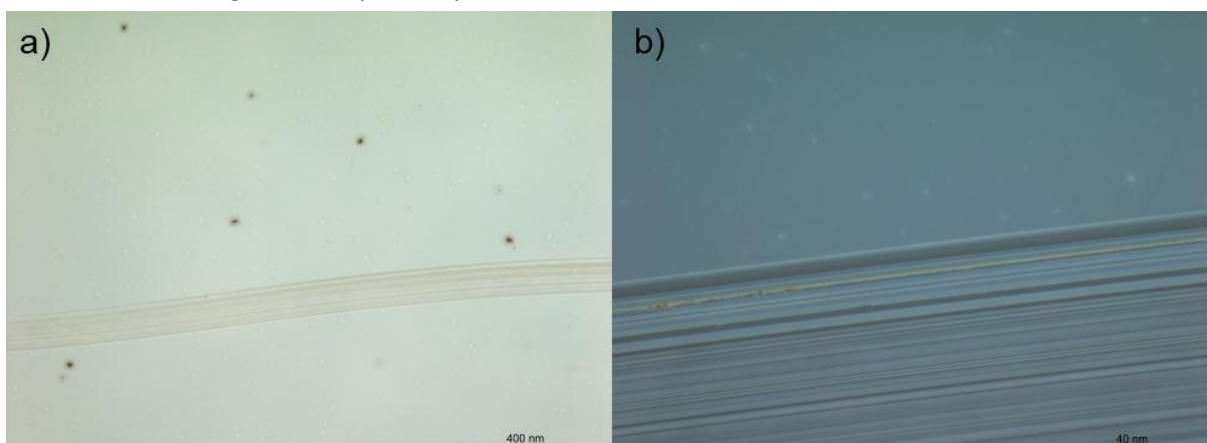


Figure 9. Microscope images of the 12.5 mg/ml, 500 rpm sample. a) Magnification: 5x. b) Magnification: 50x.

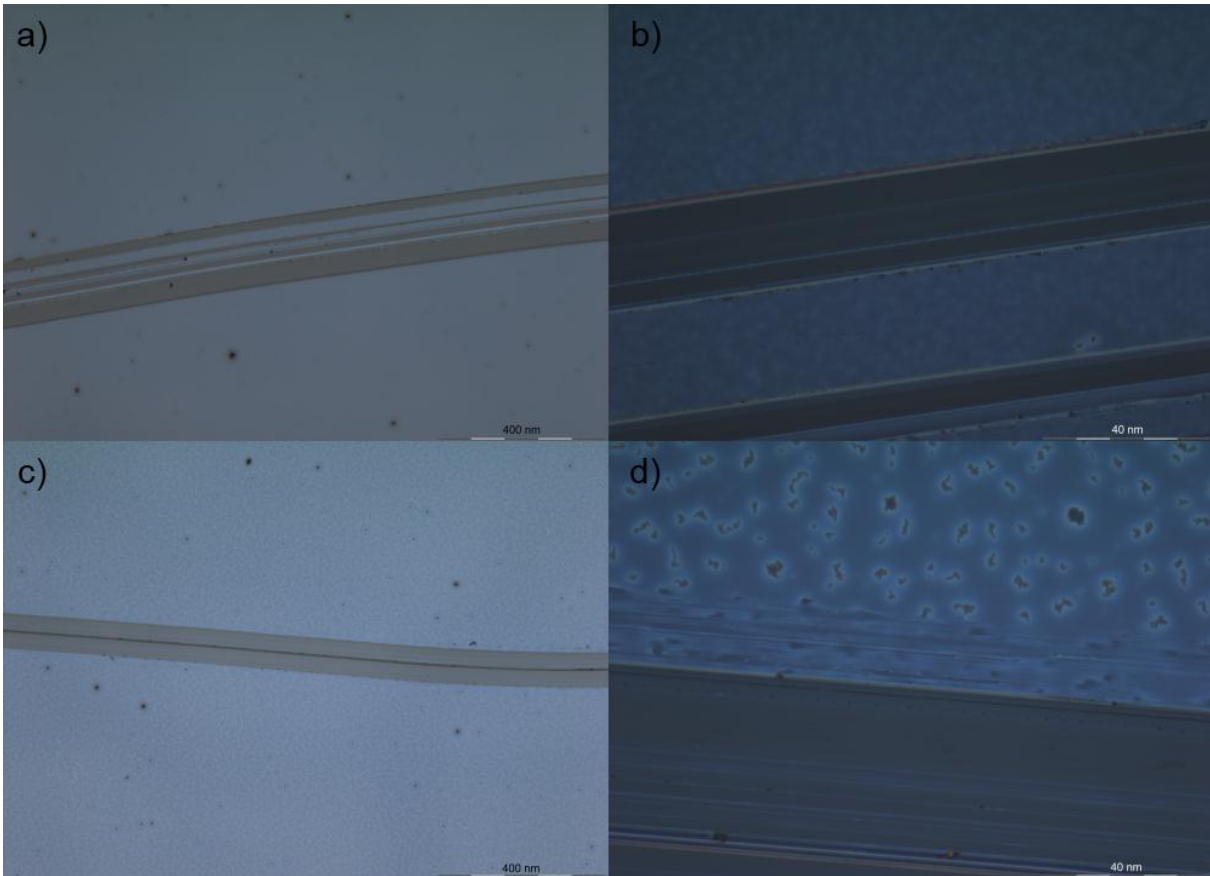


Figure 10. Microscope images of the 2% polystyrene (a,b) and the 16% polystyrene (c,d) samples, spin coated at 500 rpm. a,c) Magnification: 5x. b,d) Magnification: 50x.

thickness using the profilometer become increasingly difficult as the percentage polystyrene goes up. The layer becomes more non-uniform and discontinuous which at a certain point makes it practically impossible to perform the measurements.

Since the adding of polystyrene is apparently not helping in acquiring a better and/or thicker layer, but has only negative effects, the next step was to try heating the substrates before spin coating. The results of that are shown in figure 11. This method

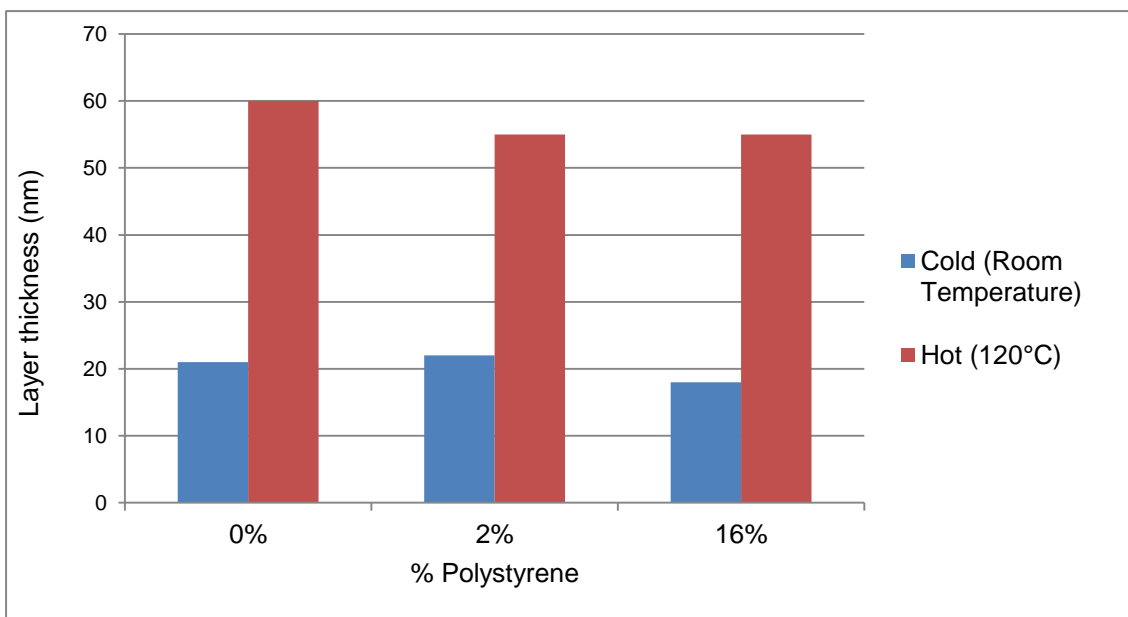
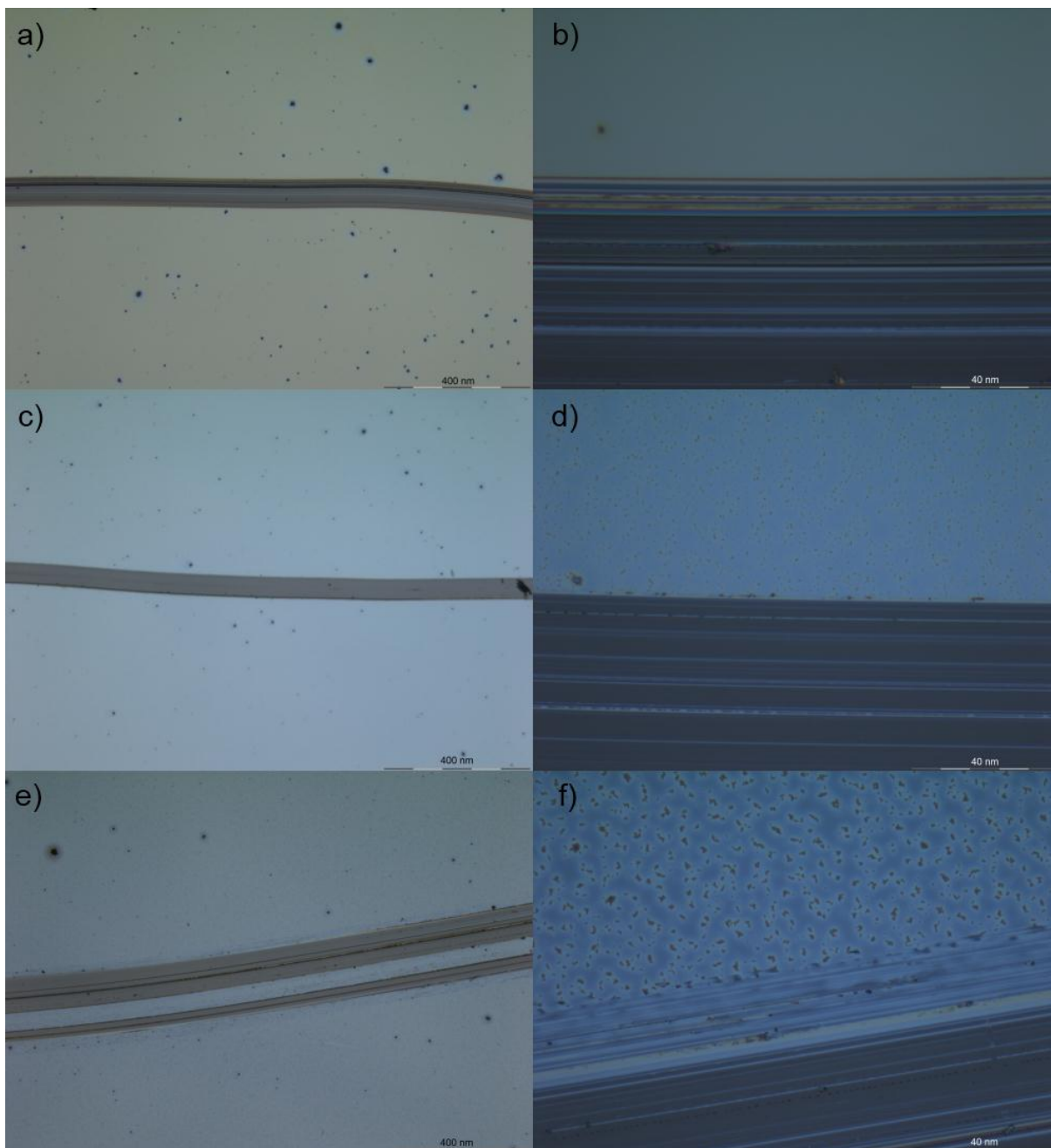


Figure 11. Comparison of layer thickness between substrates heated and substrates not heated prior to spin coating.



**Figure 12. Microscope images of the samples heated prior to spin coating (at 500 rpm), containing 0% polystyrene (a,b), 2% polystyrene (c,d) and 16% polystyrene (e,f). a,c,e) Magnification: 5x. b,d,f) Magnification: 50x.**

turned out to be remarkably effective, almost tripling the layer thickness, making it around 60 nm when using the maximum concentration of 12.5 mg/ml trans-[Fe(bapbpy)(NCS)<sub>2</sub>] in DMF, and a spinning speed of 500 rpm. This thickness is large enough to have a considerable yield when making devices. On visual inspection the spin coated layers on hot samples look different, with patches resembling coffee stains, originating from the faster evaporation of solvent near the edges of the substrate. Away

from the edges of these 'stains', the layer has roughly the same uniformity as the samples processed at room temperature. For completeness, layers from the mixed solutions with 2% and 16% polystyrene were also prepared. Here the same trend concerning the layer smoothness and uniformity was observed.

Microscope images of hot samples are included in figure 12. They closely resemble the cold samples, and adding polystyrene has the same effect as before.

### Making devices and measuring IV-characteristics

With the technique to make a significantly thick layer, devices can be fabricated to perform electrical measurements. As stated earlier, four substrates were made: two spin coated at room temperature – one mixed with 2% polystyrene, and two spin coated at 120°C – one mixed with 2% polystyrene. Performing measurements inside the probe station has resulted in the graphs in figures 13 to 15. We measured across devices of sizes 10, 20, 30, 40, 50 and 100  $\mu\text{m}$  in diameter, depending on the yield. The graphs show the current density (current divided by area) as a function of the

applied voltage. The error bars are calculated using standard deviations.

Figure 13a and 13b show the calculated averages of every hole-size, for the substrates spin coated cold and hot respectively, both containing no polystyrene. Figure 14a and 14b also show these averages for the layers spin coated on cold and hot substrates respectively, but for the solution containing 2% polystyrene. When averaged over all of the devices on a substrate, four lines are obtained, one for every wafer. These results are shown in figure 15a and 15b. The yield of the devices as a percentage can be viewed in table 2.

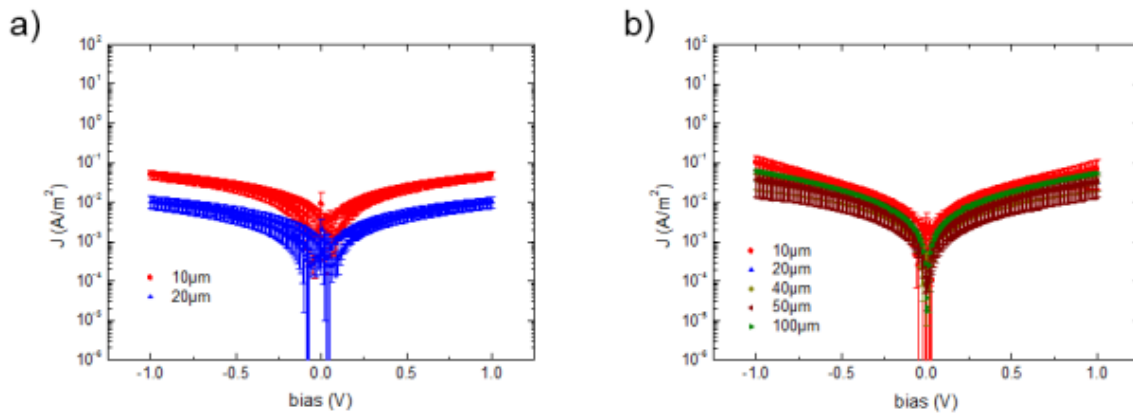


Figure 13. Current density versus the applied bias for devices with no added polystyrene. a) Cold substrate. b) Heated substrate.

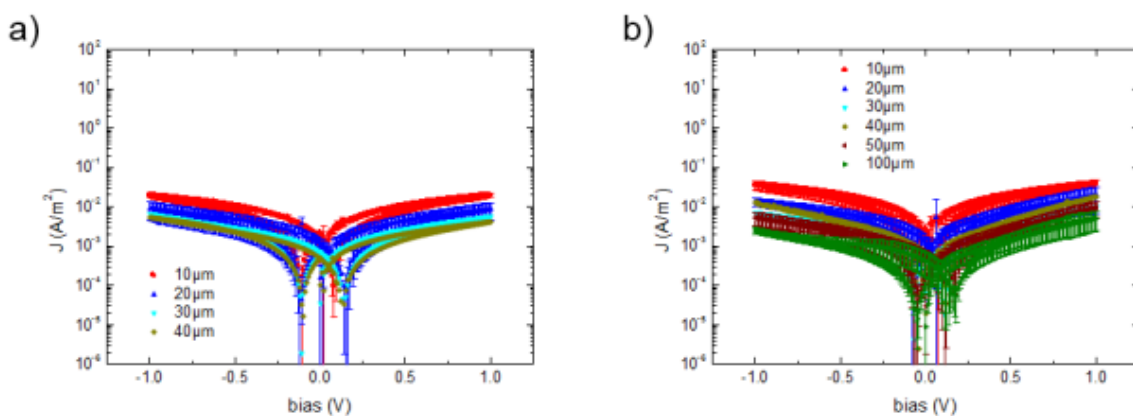


Figure 14. Current density versus the applied bias for devices with 2% polystyrene. a) Cold substrate. b) Heated substrate.

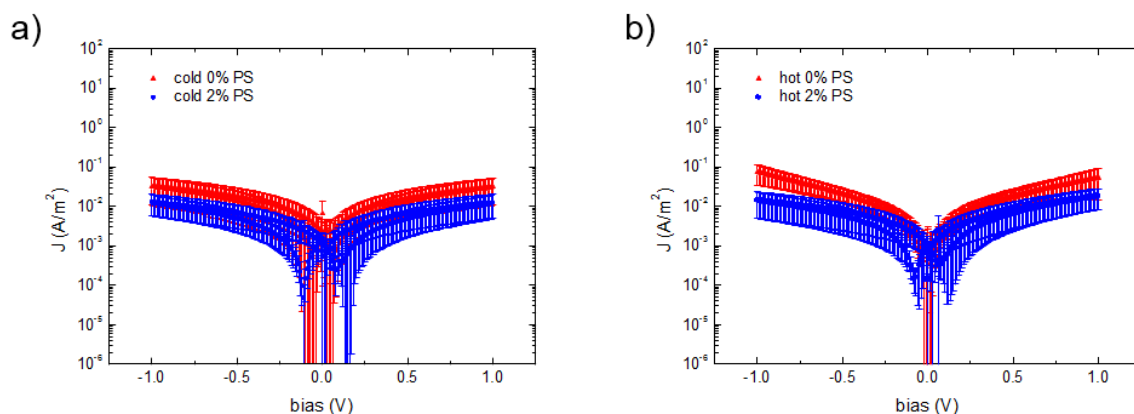


Figure 15. Current density versus the applied bias averaged over all of the devices of one substrate. a) The cold substrates, both 0% and 2% polystyrene. b) The heated substrates, both 0% and 2% polystyrene.

The observed current densities were all in the order of  $10^{-2} \text{ A/m}^2$ . With circular gaps with diameters of 10 to 100  $\mu\text{m}$ , this means that the measured currents were in the picoampère ( $10^{-12} \text{ A}$ ) range. A smaller hole area means a lower current. This also has the effect of increasing the time necessary per measurement. To conserve time, measurements of hole areas lower than 10  $\mu\text{m}$  were omitted. We recognized a shorted device by the measurement of currents approximately 5 orders of magnitude larger than those of other devices.

For the substrates spin coated without heating the substrates, it is clear from the data in table 2 that a very low yield is obtained. This can also be seen in figures 13a and 14a. We were only able to perform measurements for the devices up to 40  $\mu\text{m}$  in diameter. Devices of larger diameter were all shorted. For the devices prepared without any polystyrene no working devices were found above 20  $\mu\text{m}$ . This is probably because of the effect of the filamentary growth of the silver contact through the layer. The larger the area of the device, the higher the chance of a short circuit due to such filaments. However, the yield of the substrate without polystyrene is higher than that of the 'cold 2%' substrate. This might be another indication of the fact that adding polystyrene makes the layer less uniform, hence the correlation between device area and yield is non-trivial.

As expected, the hot samples show a considerable increase in the yield when

Table 2. The yield of each substrate

|           | Cold<br>0% | Hot<br>0% | Cold<br>2% | Hot<br>2% |
|-----------|------------|-----------|------------|-----------|
| Yield (%) | 28         | 69        | 17         | 58        |

compared to the cold samples. For both the substrates with and without polystyrene, sizes up to 100  $\mu\text{m}$  could be measured, but also here a drop in yield was observed for the substrate containing polystyrene.

The heated and non-heated substrates show roughly the same current density. This is counterintuitive, because layer thickness should be considerably influencing the conductivity of the layer. A thicker layer should result in a lower conductivity, and therefore a lower current density. The origin of this discrepancy is yet to be investigated.

The current density should in theory not depend on the area of the device, as the current is divided by this area. The graphs however, show somewhat of a spread in the currents, indicating a slight deviation from perfect scaling.

Differences between the use of polystyrene and no polystyrene can be seen in figure 15a and 15b. It is observed that the inclusion of 2% polystyrene results in a drop in the current for both the 'hot' and the 'cold' spin coated samples. This is probably stemming from the fact that polystyrene is highly resistive. Even with a low percentage as 2%, this effect is noticeable.

Hysteresis effects were not observed during the measurements. This was indeed

expected, as the transition hysteresis effects of this material were observed below room temperature. Furthermore, as the exact structure of the material in our layer is not known, it might as well be the case that trans-[Fe(bapbpy)(NCS)<sub>2</sub>], when processed using the method we developed, does not show any hysteresis effects. Magnetic susceptibility measurements are needed. For one device we tried measuring to a higher voltage range, to see if hysteresis or other effects would appear at higher biases. We increased the maximum voltage to 3.0 V for one measurement. The result is shown in figure 16. The red line shows the characteristics in the domain up to 3.0 V. No significant differences were observed, so we continued measurement using 1.0 V as a maximum, to minimize the risk of device degradation. It would be interesting to investigate the IV-characteristics as a function of temperature, so that the electrical properties can be examined at the temperature region where possible hysteresis effects could be present. However, the current decreases significantly with decreasing temperature. As the current levels at room temperature were already in the picoampère region, at low temperatures the current will be so low that the IV-curves will not be measurable. The temperature dependence was therefore not investigated.

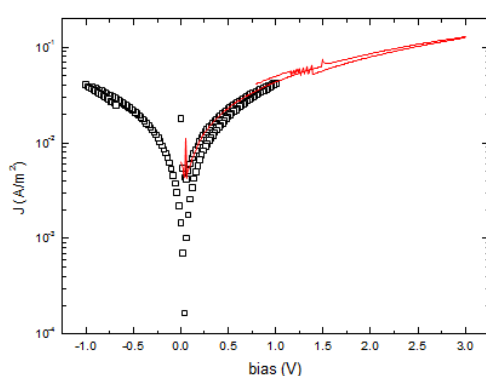


Figure 16. IV-characteristics when applying higher voltages of up to 3.0 V.

## Conclusions

The optimal method for making a layer of trans-[Fe(bapbpy)(NCS)<sub>2</sub>] is to: (I) spin coat the material dissolved in DMF at the maximum concentration of 12.5 mg/ml, (II) spin coat at the low speed of 500 rpm and (III) spin coating directly on hot substrates. This method is designed to achieve a layer that is as thick as possible. This procedure yields uniform layers of approximately 60 nm. This thickness is high enough to have considerable yield when measured in areas ranging from 10 to 100  $\mu\text{m}$ .

Adding polystyrene to the solution was tried in order to improve the layer properties and layer thickness, but turned out to have no positive effects. It is better to use only the pure material.

Although the material makes quite uniform layers, it is probably not suitable for applications as an electronic component. It has a very low conductivity and the spin transition occurs at low temperatures. A material that shows a spin transition closer to room temperature and has a higher conductivity is therefore desirable. It might also be worth focusing on polymers instead of small molecules, as they are in principle easier to process.

In a future research, it might be worth investigating the material used by F. Prins *et al.* in the large-area molecular junctions architecture.

With molecular electronic still being a relatively young field, a tremendous amount of possibilities for new applications is feasible, providing high hopes for the replacement of the inorganic semiconductors in the electrical components of the future.

## Acknowledgments

I would like to thank my two supervisors, prof. dr. Dago de Leeuw and drs. Ilias Katsouras, for allowing me to do my Bachelor research in their group. Drs. Ilias Katsouras has also taken the task to guide me throughout the course of the research, and I would like to thank him for his help and his useful ideas. I would also like to thank the rest of members of the MEPOS team for helping me with questions and

problems that occurred while working in the cleanroom.

## References

- 1 Manek Dubash, Techworld, *Moore's Law is dead, says Gordon Moore*. <http://news.techworld.com> (2005)
- 2 Robert W. Keyes, *Science*, New Series, **230**, 138 - 144 (1985)
- 3 James R. Powell, *Proceedings of the IEEE*, **96**, 1247 - 1248 (2008)
- 4 Yong Chen, Gun-Young Jung, Douglas A. A. Ohlberg, Xuema Li, Duncan R. Stewart, Jan O. Jeppesen, Kent A. Nielsen, J. Fraser Stoddart and R. Stanley Williams, *Nanotechnology*, **14**, 462 - 468 (2003)
- 5 Jonathan E. Green, Jang Wook Choi, Akram Boukai, Yuri Bunimovich, Ezekiel Johnston-Halperin, Erica Delonno, Yi Luo, Bonnie A. Sheriff, Ke Xu, Young Shik Shin, Hsian-Rong Tseng, J. Fraser Stoddart and James R. Heath, *Nature*, **445**, 414 - 417 (2007)
- 6 Ismael Díez-Pérez, Joshua Hihath, Youngu Lee, Luping Yu, Lyudmyla Adamska, Mortko A. Kozhushner, Ivan I. Oleynik and Nongjian Tao, *Nature Chemistry*, **1**, 635 - 641 (2009)
- 7 Fang Chen, Joshua Hihath, Zhifeng Huang, Xiulan Li, and N.J. Tao, *Annual Review of Physical Chemistry*, **58**, 535 - 564 (2007)
- 8 Hylke B. Akkerman, Paul W. M. Blom, Dago M. de Leeuw and Bert de Boer, *Nature*, **441**, 69 - 72 (2006)
- 9 Philipp Gütllich, Yann Garciaa and Harold A. Goodwin, *Chemical Society Reviews*, **29**, 419 - 427 (2000)
- 10 Eva Dova, *Structure Determination of Fe(II) Spin-Crossover Complexes from Powder Diffraction Data with Direct-Space Methods*, Ph.D Thesis, University of Amsterdam (2003)
- 11 Ferry Prins, Maria Monrabal-Capilla, Edgar A. Osorio, Eugenio Cornado and Herre S.J. van der Zant, *Advanced Materials*, **23**, 1545 - 1549 (2011)
- 12 Azzedine Bousseksou, Gábor Molnár, Lionel Salmon and William Nicolazzi, *Chemical Society Reviews*, **40**, 3313 - 3335 (2011)
- 13 Wikipedia, *Spin crossover*, <http://en.wikipedia.org> (accessed Jul. 2012)
- 14 Sylvestre Bonnet, Gábor Molnár, José Sanchez Costa, Maxime A. Siegler, Anthony L. Spek, Azedine Bousseksou, Wen-Tian Fu, Patrick Gamez and Jan Reedijk, *Chemistry of Materials*, **21**, 1123 - 1136 (2009)
- 15 B. T. Chen, *Polymer Engineering & Science*, **23**, 399 - 403 (1983)
- 16 Natalie Stingelin-Stutzmann, Edsger Smits, Harry Wondergem, Cristina Tanase, Paul Blom, Paul Smith and Dago de Leeuw, *Nature Materials*, **4**, 601 - 606 (2005)